Original Article

Simulation of spatiotemporal interannual variability of oceanic subsurface temperature off East Africa

Majuto C. Manyilizu[1]

[1] Department of Computer Science and Engineering, College of Informatics and Virtual Education, The University of Dodoma, P. O. Box 490, Dodoma

Western Indian Ocean JOURNAL OF Marine Science

Citation:
Manyilizu MC (2022) Simulation of spatiotemporal interannual variability of oceanic subsurface temperature off East Africa. WIO J Mar Sci 21(2): 57-70 [doi: 10.4314/wiojms.v21i2.6]

Received:
February 3, 2022

Accepted:
October 7, 2022

Published:
February 27, 2023

*** Corresponding author:**
majuto.manyilizu@udom.ac.tz

Abstract

The oceanic subsurface variability off East Africa in the tropical western Indian Ocean plays a crucial role in ocean dynamics and living resources as well as weather and climate variability. A regional ocean model is applied to understand the oceanic subsurface interannual variability off East Africa. The region with the highest sea surface temperature (SST) variability in the offshore region lies adjacent to strong subsurface temperature variations located between 30 and 130 m corresponding with strong variations in the thermocline depth. The weakest SST variations in the Tanzanian shelf waters lie over the subsurface waters with the smallest temperature variations in the upper 200 m with weak variations in the thermocline depth. Such signals are associated with induced forcings from the Indian Ocean Dipole (IOD) and El Niño-Southern Oscillation (ENSO) in both regions with different intensity and peaking times. The IOD-induced forcings are weaker, evolving in October and November-December in the region with the weakest and strongest SST variations, respectively. Relatively stronger ENSO induced forcings occur in both regions. Stronger signals occur in the region with the stongest SST variations throughout the year, except in August, with a peak in January. The ENSO-induced forcings occur in January to May peaking in March and April in the region with the weakest SST. Consequently, anomalous Rossby waves as well as local Ekman downwelling and upwelling associated with both large-scale modes occur in the region leading to the subsurface temperature variations.

Keywords: oceanic subsurface temperature, thermocline, Indian Ocean Dipole, El Niño-Southern Oscillation, downwelling, upwelling.

Introduction

The tropical Indian Ocean experiences strong interannual variability of sea surface temperature (SST) associated with internal dynamics and remote forcing resulting in significant influences towards both regional and global climate activities. Several studies have been conducted on the SST variability in the tropical Indian Ocean (e.g., Behera *et al*., 1999; Behera *et al*., 2000; Collins *et al*., 2012; Schott *et al*., 2009; Manyilizu *et al*., 2014) and a smaller number on the subsurface temperature and its relation to SST (e.g., Rao *et al*., 2002; Sun *et al*., 2021; Kakatkar *et al*., 2019, 2020; Sayantani and Gnanaseelan, 2015). The subsurface temperature in the tropical western Indian Ocean determines the vertical temperature stratification that affects upper ocean circulation, marine ecosystems and mesoscale activities in the region (Brill, 1994; Feng and Wijffels, 2002; Schott and McCreary, 2001). Furthermore, the region is part of the tropical Indian Ocean that forms the largest warm pool on Earth which shapes both regional and global warming (Schott *et al*., 2009). The recently reported break in global warming in the decadal variability in the early 21st century is associated with heat rearrangement between the surface and subsurface of the tropical Indian Ocean (Lee *et al*., 2015; Liu *et al*., 2016;

Meehl *et al*., 2011; Nieves *et al*., 2015). In the late 20th century, the tropical Indian Ocean experienced rapid surface warming aligned with the significant subsurface cooling (Han *et al*., 2006; Trenary and Han, 2008). However, such surface warming stopped in early 21st century when there was a rapid increase in subsurface warming and upper ocean heat content (Lee *et al*., 2015; Nieves *et al*., 2015). Thus, the subsurface temperature variability in the tropical Indian Ocean has peculiar features in comparison with its corresponding surface temperature.

Uniquely for the tropical Indian Ocean only, there is no co-variability between surface and subsurface spatially and temporally (Barnett *et al*., 2005; Du and Xie, 2008; Han *et al*., 2006; Nieves *et al*., 2015; Pierce *et al*., 2006; Trenary and Han, 2008) with the highest differences even opposite signatures between the trends in surface and subsurface temperatures among all oceans (Alory *et al*., 2007; Han *et al*., 2006; Nieves *et al*., 2015; Trenary and Han, 2008). For instance, the decadal variability in the subsurface temperature of the tropical Indian Ocean shows a strong seasonality with a prominent east–west dipole structure (Sun *et al*., 2021). At interannual variability scales with onsideration of the Indian Ocean Dipole (IOD) and El Niño-Southern Oscillation (ENSO) co-occurrence years, Sayantani and Gnanaseelan (2015) reported the existence of a north-south subsurface dipole in the tropical Indian Ocean. Such dipole evolves from September to November under forcing of the IOD and peaks from December through February (DJF) being reinforced by ENSO. Such patterns are maintained through March to May (MAM) of the following year. Moreover, the signals are associated with positive and negative wind stress curl anomalies in the south and north of 5°S which force downwelling and upwelling waves accordingly during the December to February period. Consequently, there is strong subsurface-surface feedback in this region which determines different surface dipole patterns apart from the commonly known of the large-scale modes; ENSO and IOD (Shinoda *et al*., 2004).

The southwestern Indian Ocean region, for example, is associated with a thermocline dome named the Seychelles Dome by Yokoi *et al*. (2008) or the Seychelles-Chagos thermocline ridge by Hermes and Reason (2008) and the shallow thermocline as reported by Manola *et al*. (2015). The variations associated with the thermocline north and south of 10°S are associated with IOD and ENSO induced forcings, respectively (e.g., Saji *et al*., 1999; Rao and Behera 2005; Yu *et al*., 2005; Tozuka *et al*., 2010; Yokoi *et al*., 2012). The SST over this region is very sensitive to thermocline variability, and hence, it can influence the regional climate variability (Chowdary *et al*., 2009; Izumo *et al*., 2008; Jayakumar *et al*., 2011; Jayakumar and Gnanaseelan, 2012; Manola *et al*., 2015; Vecchi and Harrison, 2013; Yokoi *et al*., 2008; 2012). The positive SST anomalies in this region retard the Inter-tropical convergence zone towards the Indian Subcontinent, and thus, it delays the beginning of rainfall there. Moreover, the strong SST anomalies over this region lead to strong devastating rainfall and cyclone activities over the southern Africa (Xie *et al*., 2002). Therefore, the subsurface temperature in the tropical western Indian Ocean plays a vital role in surface variability as well as shaping both regional and global climate activities; a topic of great interest recently.

The coastal waters of East Africa, as part of the tropical western Indian Ocean, indicate spatiotemporal variability of SST which greatly affects social-economic activities (such as fisheries, tourism, recreation as well as marine and coastal shipping), and ultimately, the regional economy. It mainly determines regional rainfall distribution and sea levels as well as the distribution and abundance of marine living resources (e.g., Schott *et al*., 2009; Obura *et al*., 2002). In this region, the weakest interannual SST variations which are only significant at about a five-year period, occur in the Tanzanian shelf region to the south of 6°S extending to the north and west of Madagascar. Such SST variations are predominantly influenced by the surface heat fluxes related to shortwave radiation in conjunction with a contribution from advection of the North-East Madagascar Current (NEMC) as reported by Manyilizu *et al*. (2014). The strongest interannual SST variations in the zonally elliptical band occur between 2°S and 2°N extending offshore with two significant periods of about 2.7 and 5 years (Manyilizu *et al*., 2014). These periods reflect the large-scale climate variability modes, namely ENSO (Reason *et al*., 2000; Annamalai and Murtugudde, 2004; Schott *et al*., 2009) and IOD (Behera *et al*., 2000; Yamagata *et al*., 2004), and hence suggesting their influences to such SST signals being lagged behind for two to four months (Klein *et al*., 1999; Reason *et al*., 2000; Manyilizu *et al*., 2014).

However, the subsurface temperature variability as well as its relationship with the SST in the region off East Africa are not well documented. This is due to the fact that the tropical Indian Ocean experiences the

highest differences spatially and temporally between the trends in surface and subsurface temperatures (Alory *et al*., 2007; Han *et al*., 2006; Nieves *et al*., 2015; Trenary and Han, 2008). Therefore, filling in the gaps of understanding of the subsurface temperature variability particularly the region with the weakest and strongest SST variations using numerical studies is the subject for this study. The study also explores the mechanisms behind the subsurface-surface feedbacks for the upper ocean temperature in these regions.

Datasets and methodology

The Regional Ocean Model Systems (ROMS) is used to simulate subsurface variability in the ocean off East Africa from 1980-2007. The details of the model and its configuration, datasets as well as data analysis techniques used in the study are provided below.

Model description

This study applies the ROMS which is currently improved to the Coastal and Regional Ocean Community (CROCO) model (www.croco-ocean. org) to simulate the ocean off East Africa in the tropical western Indian Ocean. Previously, this model has realistically simulated the upper ocean physical features in this region (e.g., Hermes and Reason, 2008; Penven *et al*., 2006; Manyilizu *et al*., 2014; 2016; Collins *et al*., 2014). The model is a free-surface, terrain-following ocean model which solves the three-dimensional hydrostatic primitive equations (Shchepetkin and McWilliams, 2003, 2005). It solves the equations using a split-explicit time-stepping scheme and a free-surface. Stretched, terrain-following coordinates are used in the vertical, and orthogonal curvilinear coordinates are applied in the horizontal on a staggered Arakawa C-grid. The surface heat flux is based on a bulk parameterization at the air-sea interface (Fairall *et al*., 1996). Vertical mixing occurs through the K-Profile Parameterization (KPP; Large *et al*., 1994).

The model domain setup in Manyilizu *et al*. (2014) was adapted for this study covering the region for 37.5-60°E and 4.85°N-18°S in the East African coastal waters. The study was conducted for interannual simulation forced from 1978 to 2007 with the National Center for Environmental Prediction (NCEP) reanalysis-2 of winds and heat fluxes with a two-year spin-up time. This model simulation was named as Model_NCEP. The monthly mean values were used to force the lateral open boundaries by means of a linear temporal interpolation. The lateral boundary conditions were based on a combination of active adaptive radiation conditions added to nudging (reaching a nudging time scale of 360 days) and sponge (reaching a viscosity/diffusivity value of 1000 m^2s^{-1}) layers 150 km wide (Marchesiello *et al*., 2001). With this model, the 2' spatial resolution global dataset processed by Smith and Sandwell (1997) have been configured. The model simulation has 40 vertical levels, 1/6 ° horizontal resolution and time steps of 1800s. The model outputs were averaged every two model days which in turn were processed to calculate monthly and climatological data. The monthly anomalies of the interannual model output were extracted by subtracting the monthly climatological mean calculated for 28 years (i.e., 1980-2007) of the model interpretation.

For model validation, another simulation was forced with the monthly mean Comprehensive Ocean and Atmosphere Data Sets (COADS) winds and heat fluxes (da Silva *et al*., 1994) for 10 years with a three-year spin-up time over the same domain. This model simulation was named as Model_COADS. The initial and lateral boundary conditions for this simulation were extracted from World Ocean Atlas 2001 global dataset with monthly climatology 1 ° resolution, WOA2001 (Conkright *et al*., 2002).

Datasets

Further validation of the subsurface temperature in the study region was performed using data from the observational/hydrographical World Ocean Atlas 2009 data (WOA2009). The WOA2009 consists of the global monthly climatology at 1° grid resolution and interpolated to standard depth levels on both 1° and 5° grids (Antonov *et al*., 2010; see www.nodc.noaa.gov). Thus, the model validation was conducted between the two simulations as well as data from WOA2009. Furthermore, the model configuration was validated through the SST variability using satellite and *in situ* data as shown in Figure 2 and 4 in Manyilizu *et al*. (2014).

The influences of the ENSO and the IOD on the variability of the region was assessed through correlation analysis using the Niño3.4 index and the Dipole Mode Index (DMI). The ENSO and the IOD are prominent climate modes in the tropical Indian Ocean. The DMI is provided by the Japan Agency for Marine-Earth Science and Technology (JAMSTEC) represents the difference of the monthly SST (HadISST dataset from 1958 to 2010) between two boxes in the west (50-70°E, 10°S-10°N) and the east (90-110°E, 10°S-0) of the tropical Indian Ocean (see www.jamstec.go.jp). The Niño3.4 index is extracted from the National Ocean

and Atmosphere Agency (NOAA) and is the monthly SST anomaly averaged over 5°N-5°S and 120-170°W (see gcmd.nasa.gov). It is commonly used to represent the SST variability associated with ENSO events.

Data analysis techniques

Analyses of the model results were performed using composites, correlation and Empirical Orthogonal Function (EOF) decomposition. All these techniques were applied to the monthly anomalies of the subsurface temperature and forcing variables. The correlation and standard deviations of the monthly SST anomalies were computed from the ROMS model. The possible linkage between the interannual variations of the subsurface temperature in the regions with the weakest and strongest SST was examined through correlation analysis. The EOF analysis was used to identify the leading modes of the spatiotemporal variability of the subsurface temperature in the region. The leading modes that explained more than 10% of the total variance of the subsurface temperature variability from the EOF analysis were retained.

In order to understand the subsurface temperature variations in the regions with the weakest and strongest SST variations in the ocean waters off East Africa, two transects were extracted. The first transect averaged between 1 and 1.5°S was extracted crossing the zonally elliptical band between 2°S and 2°N extending offshore. This transect represented the region with the strongest interannual SST variations that peaks at its center and it was named as the offshore region. The second transect averaged between 9 and 9.5°S. It was extracted crossing the weakest interannual SST variations which are in the Tanzanian shelf region to south of 6°S that extends to the north and west of Madagascar peaking at its center and it named as the inshore region. The selection of both transects aimed at studying the vertical subsurface temperature variations in these respectively regions. Furthermore, the transect for validation was considered around 10°S, the latitude which divides the interannual variations in two patterns as well as forcings to its north and south. The variations associated with the thermocline north and south of 10°S are associated with IOD and ENSO induced forcings, respectively (e.g., Saji *et al.*, 1999; Rao and Behera 2005; Yokoi *et al.*, 2005; Tozuka *et al.*, 2010; Yokoi *et al.*, 2012). Therefore, the vertical structure of the annual mean temperature across the domain from 38 to 60°E averaged over 10-10.5°S in the upper 250 m was used to evaluate the ability of the model to reproduce subsurface variability. This transect indicates that the ROMS model realistically simulated the subsurface temperature in the region.

Results and discussion

The tropical western Indian Ocean experiences spatial and temporal variability of subsurface temperature which does not show co-variabity with its corresponding sea surface temperture. This study focused on simulating the spatiotemporal interannual varibility of the oceanic subsurface temperature in this region off East Africa. The model validation and results of this study are provided below.

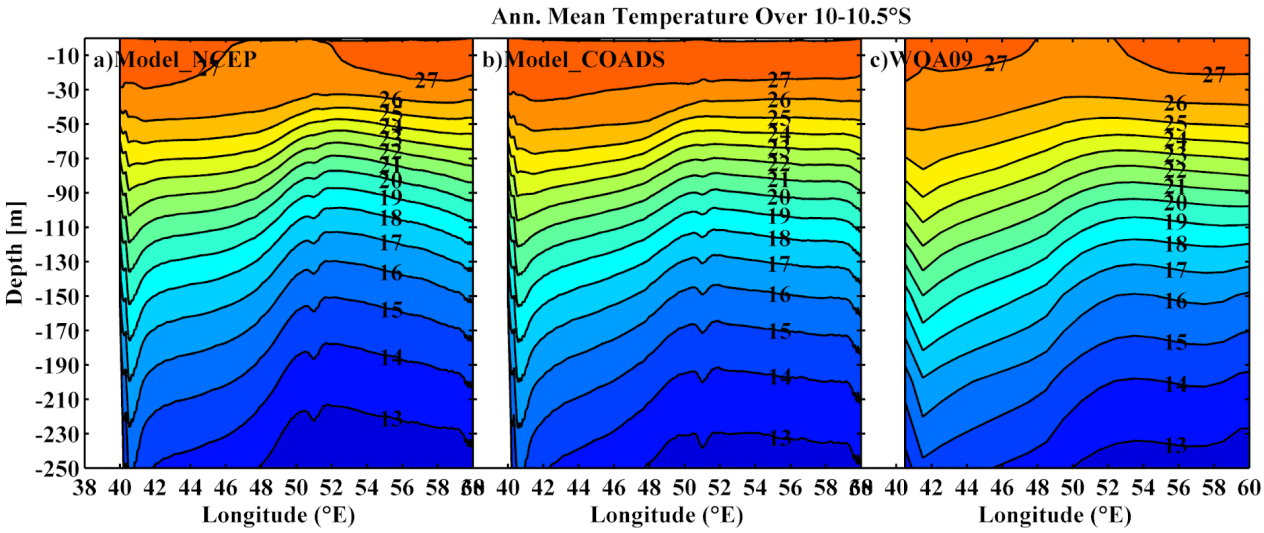

Figure 1. Annual mean of the vertical temperature in °C for Model_NCEP (1st column) and Model_COADS (2nd column), and from WOA2009 (3rd column) averaged over 10-10.5°S from 38 to 60°E with contour intervals of 1°C.

Annual subsurface temperature

The annual subsurface temperature off East Africa in the tropical western Indian Ocean is shown through a vertical transect in Figure 1. Since the 10°S latitude appears to divide north-south patterns of the interannual variability and its respective possible forcings in this region, the vertical transect around 10°S was extracted from both simulation configurations (Model_NCEP and Model_COADS) as well as from observational/ hydrographical WOA2009 data for validation.

The vertical structure of the annual mean temperature across the domain from 38 to 60°E averaged over 10-10.5°S in the upper 250 m is evaluated to understand the ability of the model to reproduce subsurface variability (Fig. 1). Relatively warm temperature (>26°C) appears in the upper 50 m in Model_NCEP and Model_COADS as well as in the WOA2009 data (Fig. 1a-c). Similar temperature patterns occur below 50 m with about 14°C isotherm laying around 250 m near the coast in both model simulations and the WOA2009 data. In short, the model seems to reproduce the annual mean of the subsurface temperature in the ocean waters off East Africa in the tropical western Indian Ocean fairly well. However, the COADS simulation shows slightly different patterns in the upper 30 m towards the sea surface. These discrepancies could be due to differences in the spatial and temporal resolutions as well as the initial and lateral boundary conditions for Model_NCEP and Model_COADS. However, the subsurface temperature variability is similarly represented in both simulations as well as in the WOA2009 data.

Therefore, the ROMS model simulated the annual mean state in the oceanic subsurface waters in this region reasonably well. This is shown by a good agreement of the mean state of the upper ocean properties from both model configurations and that from observational/ hydrographical data. Furthermore, the interannual validation of the sea surface temperature is shown in Figure 4 from Manyilizu *et al*. (2014). Thus, the next section focuses on the subsurface temperature variability in the region with the strongest SST variations.

Subsurface temperature variations off East Africa

The subsurface temperature variations in this region off East Africa were studied through the regions with the weakest and strongest SST interannual variations. The aim was to investigate the subsurface temperature signals in these regions. Thus, two transects were extracted; the first one averaged between 1 and 1.5°S crossing the zonally elliptical band between 2°S and 2°N extending offshore with the strongest interannual SST variations, and with the peak center named the offshore region. The second transect averaged between 9 and 9.5°S was extracted crossing the weakest interannual SST variations which are in the Tanzanian shelf region to the south of 6°S that extends to

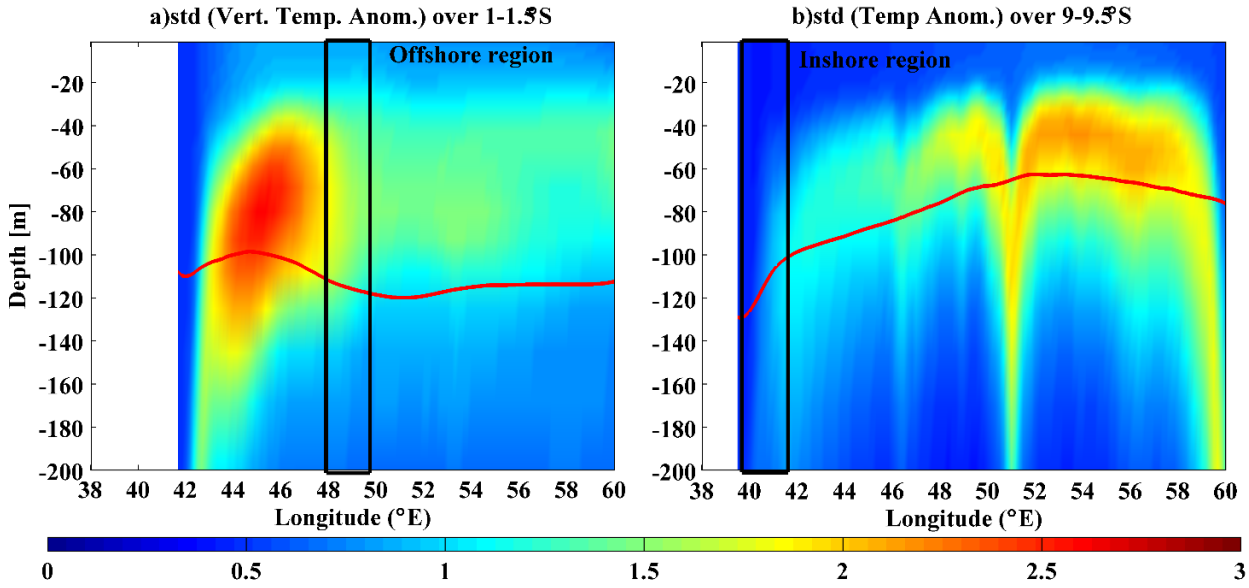

Figure 2. Standard deviation of the vertical temperature anomaly and the annual thermocline depth (red line) from 38 to 60°E averaged over (a) 1-1.5°S and (b) 9-9.5°S from 1980 to 2007 in the upper 200 m depth.

the north and west of Madagascar, with its peak center named the inshore region.

Figure 2 displays standard deviation of vertical temperature anomalies and the annual mean thermocline depth (red line) in the regions which experience the strongest and weakest interannual SST variations. The vertical transect of the standard temperature anomalies were extracted from the coast at 38 to 60°E, and averaged between 1 and 1.5°S for Figure 2a and between 9 and 9.5°S for Figure 2b from 1980 to 2007. The former transect crosses through the offshore region, and the latter one goes through the inshore region as shown in Figure 2; the regions with the strongest and weakest interannual variability of the SST, respectively.

The vertical temperature transect that crosses through the offshore region shows strong interannual temperature variations (standard deviation of about 2-3°C) in the subsurface waters between 30 and 130 m (Fig. 2a). Such patterns of subsurface temperature which show strong variations around 100 m depth were reported by Sun *et al.* (2021) and Kakatkar *et al.* (2020, 2019) as well as Sayantani and Gnanaseelan (2015). The transect displays very deep thermocline depth at the annual mean ranging from 100 to 130 m (Fig. 2a). The highest interannual variations of the vertical temperature are confined to the subsurface waters near the offshore region where the annual thermocline depth is relatively elevated. Relatively weak interannual variations of the upper ocean temperature (standard deviation <1°C) occur in the upper 30 m and below 130 m. The 130 m depth is the annual mean thermocline depth in the offshore region.

The variations of the temperature in the upper 30 m depth in the transect seems to be mainly explained by seasonality, and they are confined to the coast, where they reach below 200 m depth. The offshore region corresponds to strong interannual variations in the thermocline depth with a standard deviation which ranges from 18 m at 50°E to 24 m at 48°E (Fig. 3). Consequently, variations in the thermocline depth are associated with strong variations in the upper temperature in the offshore region.

The vertical temperature transect through the coastal waters in the Tanzanian shelf region shows weak interannual variations (standard deviation <0.5°C) in the upper 200 m depth (Fig. 2b). The annual mean of the thermocline depth ranges from 70-80 m in the Seychelles-Chagos thermocline ridge as reported by Hermes and Reason (2008) and Yokoi *et al.* (2008) to the deepest value (130 m) in the Tanzanian shelf region. In this transect, strong seasonality is present in the upper 40 m (explained variance >80% not shown), and it is confined to the coast where it reaches below 200 m. High subsurface temperature variations (standard deviations of about 1.5-2.0°C) occur between 30 and 80 m to the east of the transect which seems to advect towards the Tanzanian shelf region. These high subsurface temperature variations are located between 48 and 60°E. The region corresponds with relatively high standard deviation of the thermocline depth (>13 m) which becomes higher than that in the offshore region

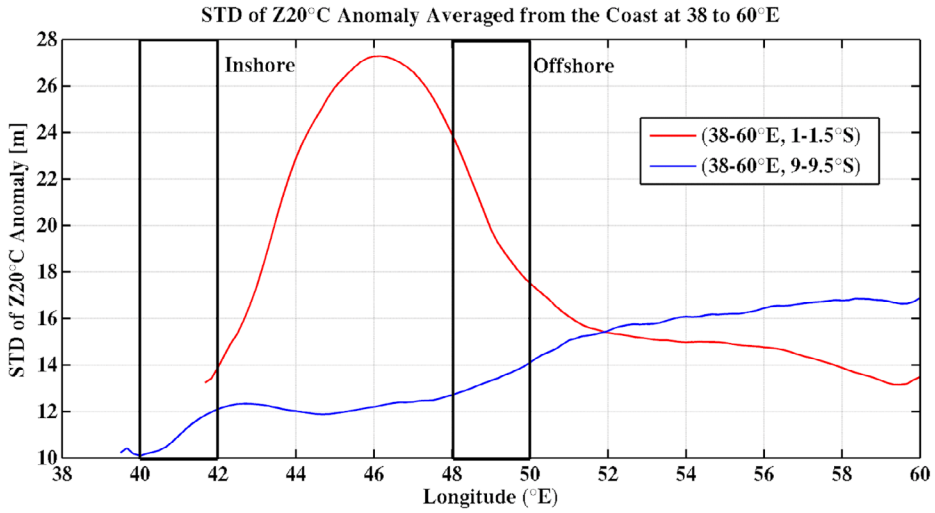

Figure 3. Standard deviation of the thermocline anomalies from the ROMS model in the tropical western Indian Ocean averaged from the coast at 38 to 60°E over 1-1.5°S (red) and 9-9.5°S (blue).

towards the east of 52°E (>15 m). This region reflects the thermocline dome named the Seychelles Dome by Yokoi *et al*. (2008) or Seychelles-Chagos thermocline ridge by Hermes and Reason (2008); the shallow thermocline also reported by Manola *et al*. (2015). Thus, uniformly weak variations of the temperature in the upper 200 m occur in the Tanzanian shelf region which is mainly dominated by seasonality and some contribution from advection from the region with high variations to the east in the subsurface waters.

In general, the region with the highest SST variability in the offshore region lies adjacent to strong subsurface temperature variations located between 30 and 130 m. Moreover, the region corresponds with strong variations in the thermocline depth. The weakest SST variations in the Tanzanian shelf waters lie over the subsurface waters with the smallest temperature variations in the upper 200 m. It matches with weak variations in the thermocline depth. The highest regional variability of the subsurface temperature is further explained by interannual variability. Thus, the next section deals with subsurface temperature in the region in association with large-scale climate variability modes.

Subsurface temperature with large-scale climate variability modes

An Empirical Orthogonal Function (EOF) analysis was applied to the upper ocean temperature (0-200 m depth) in the vertical transects through the Tanzanian shelf region and offshore in the tropical western Indian Ocean off East Africa. The analysis was performed on the monthly vertical temperature anomalies to determine the dominant modes of variability.

Vertical interannual temperature variability through the region with the weakest SST variations

The EOF analysis in the transect through the region with the weakest SST variations in the Tanzanian shelf waters was performed on the monthly vertical temperature anomalies from 38 to 60°E averaged between 9 and 9.5°S from 1980 to 2007 (Fig. 4). The first two leading modes of the vertical temperature anomalies in the upper 200 m of the EOF, which collectively explain about 64% of the total variance, were retained.

The first mode explains about 51% of the total variance with the same sign everywhere in the transect (Fig. 4a). The weakest loadings are in the Tanzanian shelf region reflecting the weakest temperature

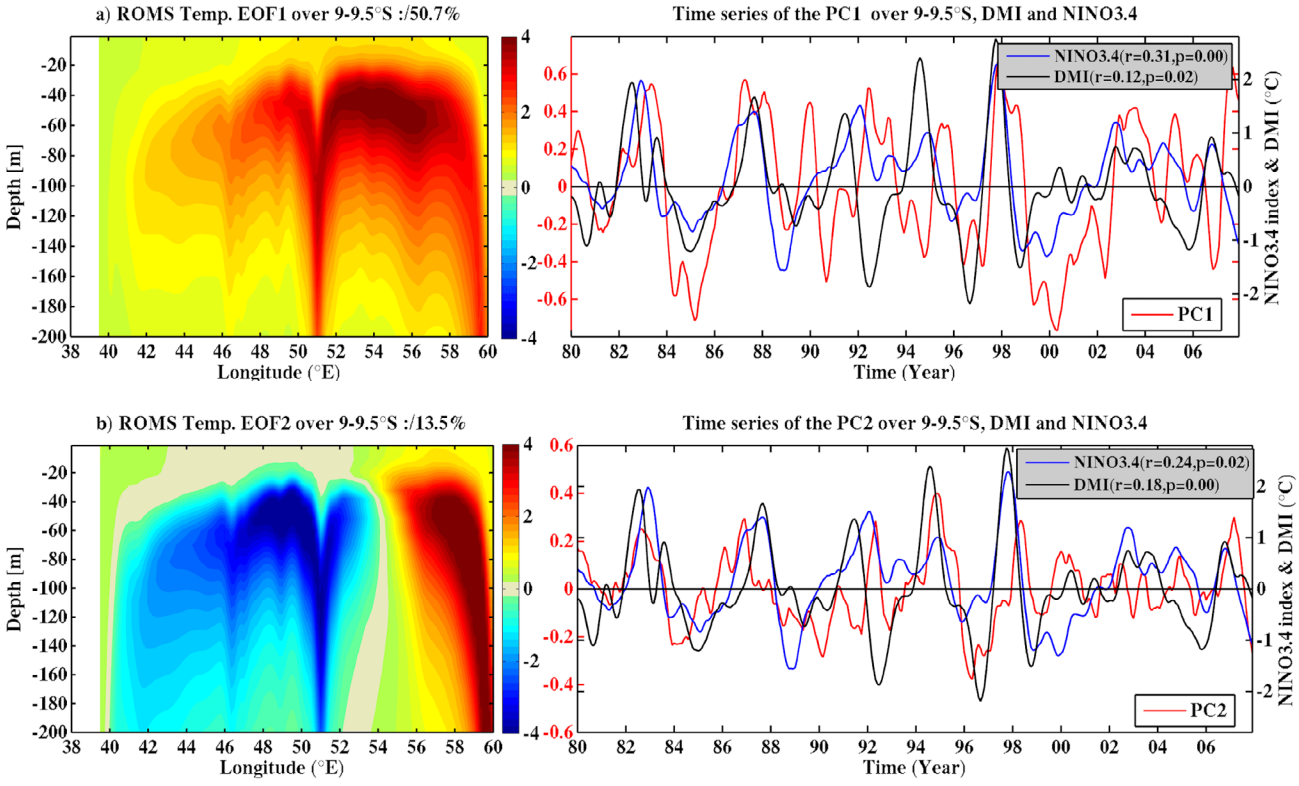

Figure 4. The first two EOF modes for the upper ocean temperature (0-200 m) from 38 to 60°E averaged over 9-9.5°S and their corresponding principal component time series (in red). The DMI (in black) and the Niño3.4 index (in blue) are added. The time series is smoothed by a seven-month running mean. (a) 1st EOF, (b) 2nd EOF.

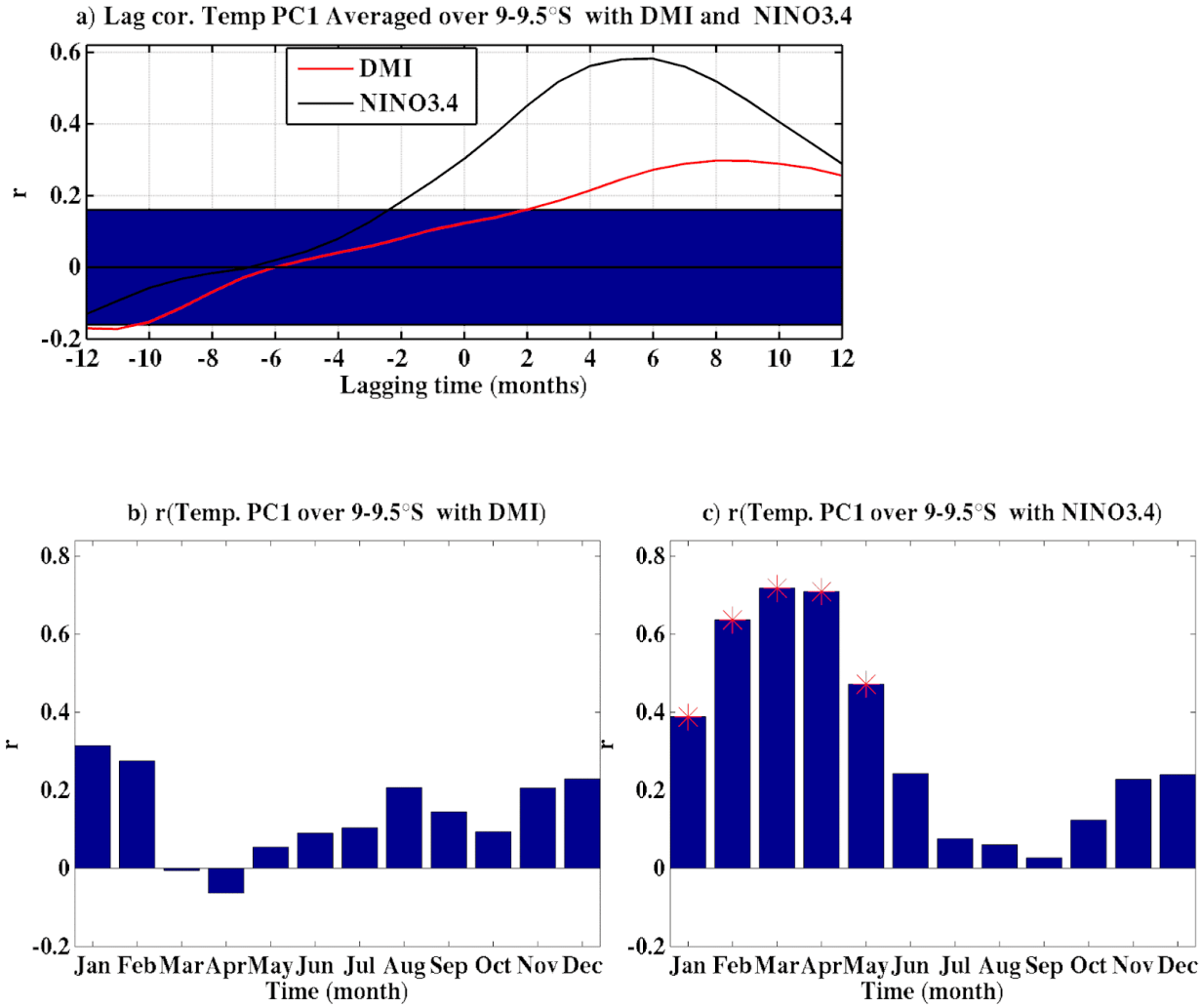

Figure 5. (a) Lag correlation of the Niño3.4 index (black) and the DMI (red) with the PC1 of the vertical temperature EOF from 38 to 60°E averaged over 9-9.5°S in the upper 200 m. Bar diagrams of the monthly correlation coefficients between the PC1 with (b) the DMI (left) and (c) the Niño3.4 index (right). The unshaded region in (a) and the red stars in (b) and (c) indicate statistically significant correlation at 95% significant levels (p<=0.05).

variations. However, strong spatial loading patterns occur to the east between 48 and 60°E in the subsurface waters between 20 to 140 m where they match with strong standard deviation in the vertical temperature anomalies. Such loadings reflect those of the Seychelles Dome (Yokoi *et al.*, 2008) or Seychelles-Chagos ridge (Hermes and Reason, 2008), the shallow thermocline also reported by Manola *et al.* (2015). The principal component time series of the first EOF (PC1) of the anomalies in the upper temperature correlates with the Niño3.4 index and the DMI with values of 0.31 and 0.12 at 95% significant level, respectively. Such findings suggest a relatively stronger influence of the ENSO than the IOD with the IOD and ENSO-induced Rossby waves dominating to the north and south of 10°S, respectively (Rao *et al.*, 2005; Yu *et al.*, 2005).

The second mode of the EOF analysis explains about 14% of the total variance with an east-west dipole spatial pattern in the subsurface waters (Fig. 4b). The lowest values close to zero occur in the upper 30 m being confined to the Tanzanian shelf region. The PC2 shows correlation with the Niño3.4 index and the DMI with values of about 0.24 and 0.18 at 95% significant levels, respectively. The first two modes of the monthly vertical temperature anomalies through the Tanzanian shelf waters show correlation with ENSO and IOD signals. Very low and relatively high values of correlation between the large-scale indices (Niño3.4 index and DMI) occur with the upper temperature in the Tanzanian shelf region and offshore, respectively. However, significantly small values of correlation of the PC1 and PC2 with the Niño3.4 index and the DMI

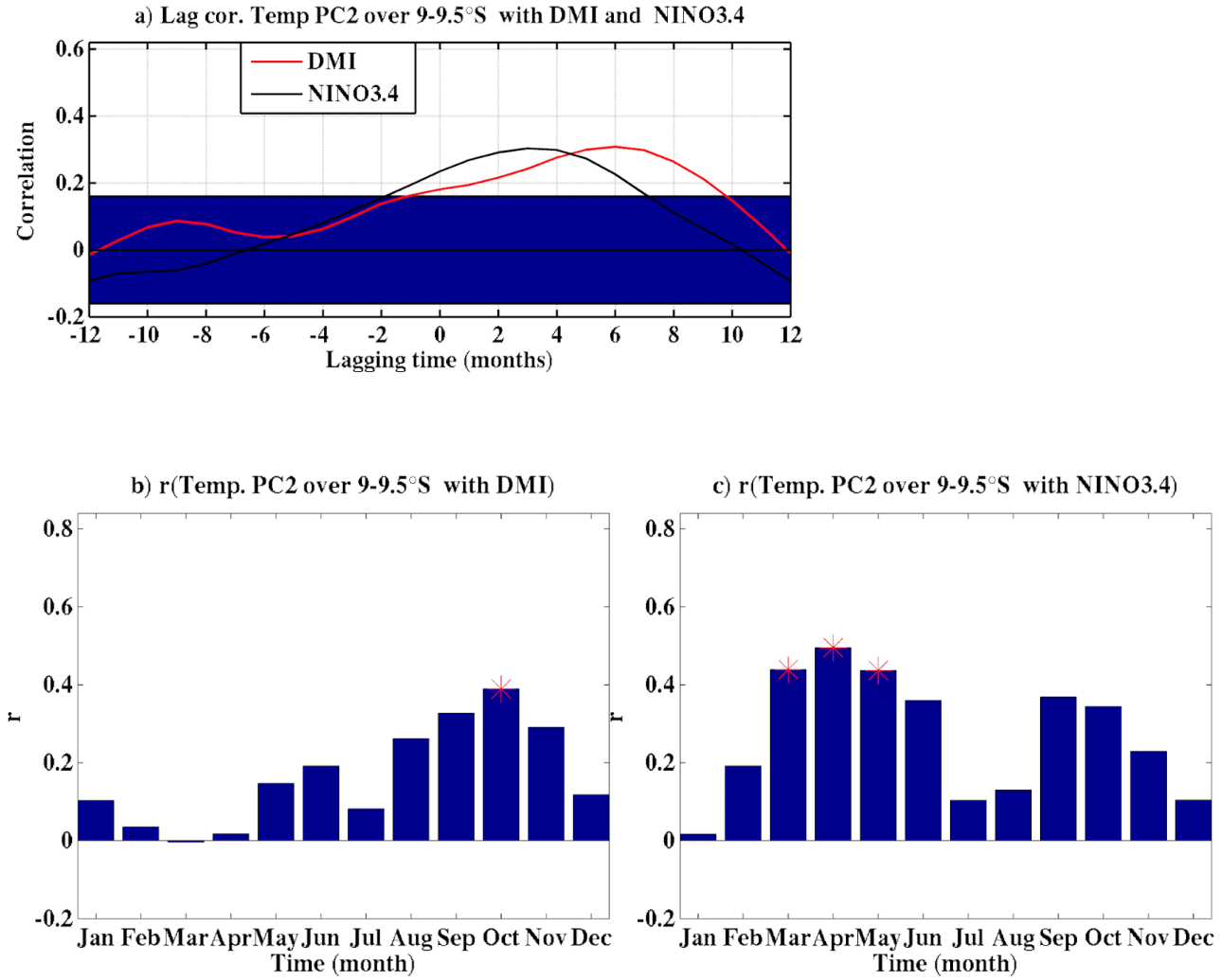

Figure 6. (a) Lag correlation of the Niño3.4 index (black) and the DMI (red) with the PC2 of the vertical temperature EOF from 38 to 60°E averaged over 9-9.5°S in the upper 200 m. Bar diagrams of the monthly correlation coefficients between the PC2 with (b) the DMI (left) and (c) the Niño3.4 index (right). The unshaded region in (a) and the red stars in (b) and (c) indicate statistically significant correlation at 95% significant levels (p<=0.05).

could be associated with strong seasonality of the indices. Thus, stratification of the PC1 and PC2 as well as their correlation with the Niño3.4 index and the DMI in calendar months can provide strong correlation in seasonal variations.

To understand the seasonal variations of the vertical temperature anomalies in the Tanzanian shelf region and their relation to the ENSO and IOD signals, the principal component time series of the first two leading modes and their correlation with the Niño3.4 index and the DMI were stratified by calendar months. The PC1 of the vertical temperature anomalies in the region mostly correlated with the Niño3.4 index (r>0.6) at a 95% significant level when the Niño3.4 index lags behind the PC1 by 3-7 months (Fig. 5a). However, the correlation between the PC1 of the vertical temperature anomalies with the DMI is very weak. Furthermore, no significant monthly correlation exists between PC1 of the vertical temperature anomalies and the DMI (Fig. 5b). On the other hand, the Niño3.4 index and the PC1 of the vertical temperature anomalies show a strong correlation from January to April, peaking in March-April at about 0.7 (Fig. 5c). Such findings appear to capture the influence of the ENSO in the subsurface temperature in the region reported to be in December-February which might be maintained to the following March-May season (Shidona *et al.*, 2004; Sayantani and Gnanaseelan, 2015). Weak signals of the ENSO and IOD appear in the PC2 of the vertical temperature anomalies which are relatively weakly correlated (r~=0.3) when the Niño3.4

index and the DMI lags behind the PC2 by 2-3 and 5 months, respectively (Fig. 6a). No significant monthly correlation of the PC2 with the DMI exists except in October (r~=0.4; Fig. 6b). The combination of the seasonal influences of the ENSO and IOD signals reflects the analysis of Sayantani and Gnanaseelan (2015) that the IOD influences the subsurface variations in the September-November (SON) season being intensified by the ENSO from December to February and retained through March to May. These results suggest strong variations of the interannual vertical temperature anomalies around 9-9.5°S in the tropical western Indian Ocean are more associated with ENSO signals than IOD signals as was previously reported by Rao *et al.* (2005) and Yu *et al.* (2005).

Vertical interannual temperature variability in the region with the strongest SST variations

The monthly temperature anomalies of the vertical transect through the offshore region are used to compute the EOFs in the region from 38 to 60°E averaged between 1 and 1.5°S. The first leading mode of the vertical temperature of the EOF which explains about 52% of the total variance with a homogeneous signal of the spatial pattern is retained (Fig. 7). Strong spatial loading patterns occur between 20 and 160 m depth matching the strong variations in temperature. The offshore region appears to the east of the strongest loadings in this EOF with upward advection toward the surface waters. The PC1 of the upper temperature anomalies correlate with the Niño3.4 index and the DMI with values of 0.58 and 0.21 at 95% significant level, respectively. Therefore, the vertical temperature anomalies in the offshore region between 48 and 50° E and the nearby are associated with the ENSO and the IOD signals. Moreover, significant correlation of the PC1 with the Niño3.4 index and DMI could be obtained if they are stratified in calendar months due to the fact that the ENSO and IOD signals in the tropical Indian Ocean are annually phase-locked.

Figure 8 displays the standard deviation of the monthly PC1 through the offshore region from 38 to 60°E averaged between 1 and 1.5°S for the vertical temperature anomalies stratified in calendar months. The PC1 shows relatively strong standard deviation from August to December which peaks in December at about 0.4°C. The vertical temperature anomalies in this region mostly correlate with the Niño3.4 index (r=~0.6) at 95% significant level when the Niño3.4 index lags behind the PC1 by 1-3 months. Moreover, the correlation between the PC1 of the vertical temperature anomalies in the region with the DMI peaks at 2-4 lag months. Monthly correlation of about 0.42 appears between the PC1 of the vertical temperature anomalies and the DMI in only December at the 95% significant level (Fig. 8b). However, the Niño3.4 index and the PC1 of the vertical temperature anomalies show significantly strong correlation throughout the year, except in August, and the correlation peaks in January at about 0.8 (Fig. 8c). Such patterns could be explained by the analysis of Sayantani and Gnanaseelan (2015) who showed that the subsurface temperature in the tropical Indian Ocean evolves from September to November forced with the IOD, intensifying and peaking in the following season in December–February (DJF), being reinforced by ENSO. Such patterns are maintained through March–May (MAM) of the following year.

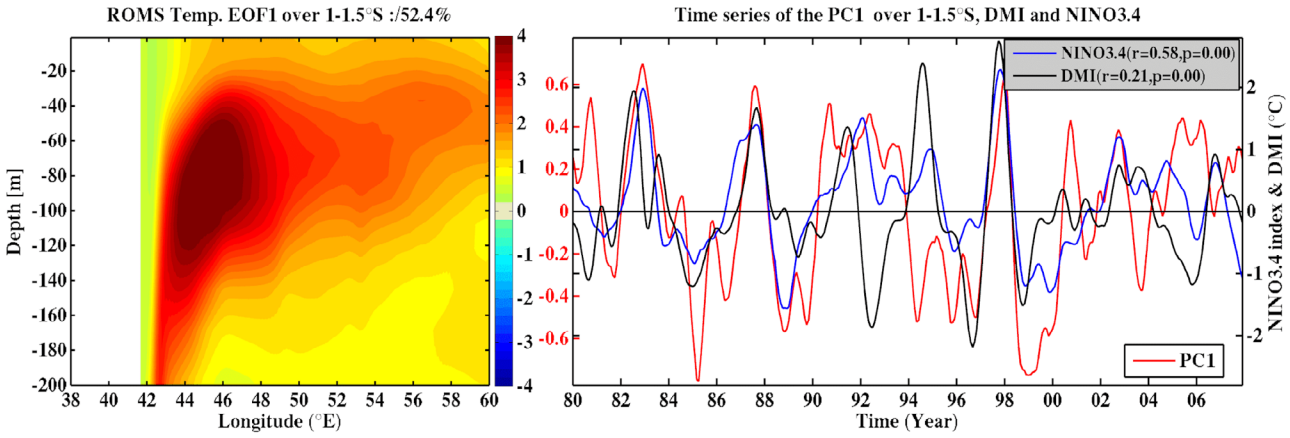

Figure 7. The first EOF mode for the upper ocean temperature (in 200 m depth) from 38 to 60°E averaged over 1-1.5°S in tropical western Indian Ocean and their corresponding principal component time series (in red). The DMI (in black) and the Niño3.4 index (in blue) are added. The time series is smoothed by a seven-month running mean.

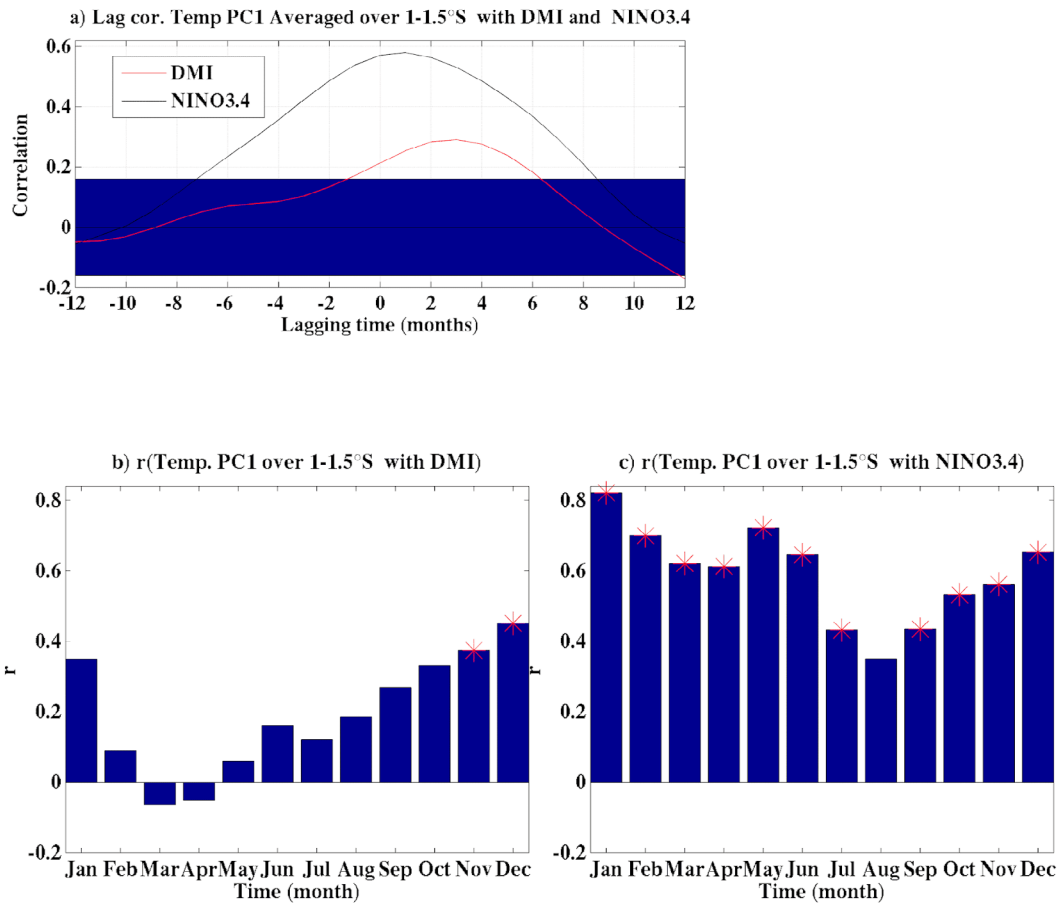

Figure 8. (a) Lag correlation of the Niño3.4 index (black) and the DMI (red) with the PC1 of the vertical temperature EOF from 38 to 60°E averaged over 1-1.5°S in the upper 200 m. Bar diagrams of the monthly correlation coefficients between the PC1 with (b) the DMI (left) and (c) the Niño3.4 index (right). The unshaded region in (a) and the red stars in (b) and (c) indicate statistically significant correlation at 95% significant levels (p<=0.05).

In the Sayantani and Gnanaseelan (2015) study, the patterns were linked with positive and negative wind stress curl anomalies in the south and north of 5°S which force downwelling and upwelling waves respectively during the December-February period. Therefore, there is strong subsurface-surface feedback in the tropical Indian Ocean which determines different surface dipole patterns apart from the commonly known large scale modes of ENSO and IOD (Shinoda *et al.*, 2004). It is apparent that strong variations of the interannual temperature in the upper 200 m which are related to the thermocline variations in the offshore region are associated mainly with the ENSO and IOD signals.

Summary and conclusion

The ROMS which has been improved into the CROCO model was used to simulate the oceanic subsurface temperature off East Africa in the tropical western Indian Ocean. The study focused on understanding the subsurface variations in the regions with the strongest and weakest SST variations in the region from 1980 to 2007. The ability of the model to reproduce the variability in this region is reasonable as the model outputs are in good agreement with observations and hydrographical data.

The upper ocean temperature in the tropical western Indian Ocean showed spatial and temporal variability. The offshore region around 48-50°E averaged between 1 and 1.5°S showed high interannual temperature variability in the upper 200 m. Weak inter-annual variations of the vertical temperature anomalies occur in the Tanzanian shelf region in the upper 200 m. The region experiences weak inter-annual variations in the thermocline suggesting that local forcing is responsible for the variability. However, strong variability in the thermocline to the east of the Tanzanian shelf waters leads to strong subsurface inter-annual variability which could influence the Tanzanian shelf

region at that depth through advection. The offshore region experiences strong inter-annual variability in the vertical temperature with the highest variability between 30 and 130 m depth. The regional variability of the subsurface temperature cannot be explained by seasonality, and thus, it is related to modes of inter-annual variability. Strong inter-annual variability in the thermocline depth associated with the local surface forcing and the remote forcing from ENSO and the IOD is responsible for the strong inter-annual variability in the region. The strongest inter-annual variability in the mid depth between 40 and 130 m seems to be upwelled towards the surface. Therefore, surface and subsurface temperatures in the Tanzanian shelf region vary in the same way with weak inter-annual variability. However, stronger inter-annual variability of the temperature occurs in the subsurface waters than in the SST in the offshore region. The strong variability in the offshore region is related to strong inter-annual variability in the thermocline associated with the ENSO and the IOD.

This study provides an understanding of the subsurface temperature variability in relation to the SST in the tropical western Indian Ocean; factors that are very important for climate and marine living resources. Such understanding improves planning and management of climate sensitive activities in the East African marine ecosystem region and marine shipping activities in the Tanzanian shelf region.

To summarize, the upper ocean temperature in the tropical western Indian Ocean shows spatial and temporal variability. The offshore region around 48-50°E averaged between 1 and 1.5°S shows high interannual temperature variability in the upper 200 m. The highest temperature variations are confined to the subsurface, and they match with anomalous thermocline depths. Moreover, the subsurface temperature variations in the offshore region strongly relate to the ENSO and IOD. The Tanzanian shelf region indicates weak temperature variations in the upper 200 m with weak influences of ENSO and the IOD.

Acknowledgments

The numerical model data for this study can be obtained by contacting the corresponding author, Majuto Manyilizu (via email address: majuto.manyilizu@udom.ac.tz or majuto.manyilizu@gmail.com). The WOA2009 data are accessed through www.nodc.noaa.gov. The DMI is provided by the Japan Agency for Marine-Earth Science and Technology (JAMSTEC) on www.jamstec.go.jp and the Niño3.4 index is extracted from National Ocean and Atmosphere Agency (NOAA) through gcmd.nasa.gov. Special thanks to the Carnegie-IAS Regional Initiative in Science and Education (RISE) through the western Indian Ocean Regional Initiative in Marine Science and Education (WIO-RISE) network for funding this research.

References

Alory G, Wijffels S, Meyers G (2007) Observed temperature trends in the Indian Ocean over 1960–1999 and associated mechanisms. Geophysical Research Letters 34: L02606 [doi.org/10.1029/2006GL028044]

Annamalai H, Murtugudde R (2004) The role of the Indian Ocean in regional climate variability. Ocean-Atmosphere Interaction and Climate Variability, Geophysical Monograph Series 147. American Geophysical Union: 210-250 [https://doi.org/10.1029/147GM13]

Antonov JI, Seidov D, Boyer TP, Locarnini RA, Mishonov AV, Garcia HE, Baranova OK, Zweng MM, Johnson DR (2010) World Ocean atlas 2009 vol. 2, Salinity. In: Levitus S (ed) NOAA Atlas NESDIS 69. NOAA, Silver Spring, Md. 184 pp

Barnett TP, Pierce DW, AchutaRao KM, Gleckler PJ, Santer B.D, Gregory JM, Washington WM (2005) Penetration of human-induced warming into the world's oceans. Science 309: 284-287 [doi.org/10.1126/science.1112418]

Behera SK, Krishnan R, Yamagata T (1999) Unusual ocean-atmosphere conditions in the tropical Indian Ocean during 1994. Geophysical Research Letters 26: 3001-3004 [doi: 10.1029/1999GL010434]

Behera SK, Salvekar PS, Yamagata T (2000) Simulation of inter-annual SST variability in the tropical Indian Ocean. Journal of Climate 13: 3487-3499 [doi: https://doi.org/10.1175/1520-0442(2000)013<3487:SOISVI>2.0.CO;2]

Brill RW (1994) A review of temperature and oxygen tolerance studies of tunas pertinent to fisheries oceanography, movement models and stock assessments. Fishery Oceanography 3: 204-216 [doi.org/10.1111/j.1365-2419. 1994.tb00098.x]

Chowdary JS, Gnanaseelan, C, Xie SP (2009) Westward propagation of barrier layer formation in the 2006–07 Rossby wave event over the tropical southwest Indian Ocean. Geophysical Research Letters 36: L04607 [doi.org/10.1029/2008GL036642]

Collins C, Reason CJC, Hermes JC (2012) Scatterometer and reanalysis wind products over the western tropical Indian Ocean. Journal of Geophysical Research 117: C03045 [https://doi.org/10.1029/2011JC007531]

Collins C, Hermes JC, Reason CJC (2014) Mesoscale activity in the Comoros Basin from satellite altimetry and

a high-resolution ocean circulation model. Journal of Geophysical Research 119: 4745-4760 [https://doi.org/10.1002/2014JC010008]

Conkright ME, Locarnini RA, Garcia HE, O'Brien TD, Boyer TP, Stephens C, Antonov JI (2002) World ocean atlas 2001: Objective analyses, data statistics, and figures, CD-ROM documentation. Technical report, National Oceanographic Data Center, Silver Spring, MD

da Silva AM, Young CC, Levitus S (1994) Atlas of surface marine data 1994, vol. 1: Algorithms and procedures. Technical report 6, United States Department of Commerce, NOAA, NESDIS

Du Y, Xie SP (2008) Role of atmospheric adjustments in the tropical Indian Ocean warming during the 20th century in climate models. Geophysical Research Letters 35 (8): L08712 [doi.org/10.1029/2008GL033631]

Fairall CW, Bradley EF, Rogers DP, Edson JB, Young GS (1996) Bulk parameterization of air-sea fluxes for TOGA COARE. Journal of Geophysical Research 101: 3747-3764 [doi: 10.1029/95JC03205]

Feng M, Wijffels S (2002) Intraseasonal variability in the south equatorial current of the East Indian Ocean. Journal of Physical Oceanography 32: 265-277 [doi.org/10.1175/1520-0485(2002)0322.0.CO;2]

Han W, Meehl GA, Hu A (2006) Interpretation of tropical thermocline cooling in the Indian and Pacific oceans during recent decades. Geophysical Research Letters 33 (23): L23615 [doi. org/10.1029/2006GL027982]

Hermes JC, Reason CJC (2008) Annual cycle of the South Indian Ocean (Seychelles-Chagos) thermocline ridge in a regional ocean model. Journal of Geophysical Research 113: C04035 [doi: 10.1029/2007JC004363]

Izumo T, Montégut CB, Luo JJ, Behera SK, Masson S, Yamagata T (2008) The role of the Western Arabian Sea upwelling in Indian Monsoon Rainfall variability. Journal of Climatology 21: 5603-5623 [doi.org/10.1175/2008JCLI2158.1]

Jayakumar A, Vialard J, Lengaigne M, Gnanaseelan C, McCreary JP, Kumar BP (2011) Processes controlling the surface temperature signature of the Madden-Julian Oscillation in the thermocline ridge of the Indian Ocean. Climate Dynamics 37: 2217–2234 [doi.org/10.1007/s00382-010-0953-5]

Jayakumar A, Gnanaseelan C (2012) Anomalous intraseasonal events in the thermocline ridge region of Southern Tropical Indian Ocean and their regional impacts. *Journal of Geophysical Research: Oceans* 117: C03021 [doi.org/10.1029/2011JC007357]

Kakatkar R, Gnanaseelan C, Chowdary JS, Deepa JS, Parekh A (2019) Biases in the tropical Indian Ocean subsurface temperature variability in a coupled model. *Climate Dynamics* 52: 5325-5344 [doi.org/10.1007/s00382-018-4455-1]

Kakatkar R, Gnanaseelan C, Chowdary JS (2020) Asymmetry in the tropical Indian Ocean subsurface temperature variability. Dynamics of Atmospheres and Oceans 90: 101142 ISSN [0377-0265] [doi.org/10.1016/j.dynatmoce.2020.101142]

Klein SA, Soden BJ, Lau NC (1999) Remote Sea surface temperature variations during ENSO: Evidence for a tropical atmospheric bridge. Journal of Climate 12: 917-932 [doi: https://doi.org/10.1175/1520-0442(1999)012<0917:RSSTVD>2.0.CO;2]

Large WG, McWilliams JC, Doney SC (1994) Oceanic vertical mixing: a review and a model with a non-local boundary layer parameterization. Reviews of Geophysics 32: 363-403 [https://doi.org/10.1029/94RG01872]

Lee SK, Park W, Baringer MO, Gordon AL, Huber B, Liu Y (2015) Pacific origin of the abrupt increase in Indian Ocean heat content during the warming hiatus. Nature Geoscience 8: 445 [doi.org/10.1038/ngeo2438]

Liu W, Xie SP, Lu J (2016) Tracking ocean heat uptake during the surface warming hiatus. Nature Communications 7: 10926 [doi.org/10.1038/ncomms10926]

Manola I, Selten FM, de Ruijter WPM, Hazeleger W (2015) The ocean-atmosphere response to wind-induced thermocline changes in the tropical South Western Indian Ocean. Climate Dynamics 45: 989–1007 [doi.org/10.1007/s00382-014-2338-7]

Manyilizu M, Dufois F, Penven P, Reason C (2014) Inter-annual variability of sea surface temperature and circulation in the tropical western Indian Ocean. African Journal of Marine Science 36 (2): 233-252 [doi:10.2989/1814232X.2014.928651]

Manyilizu M, Penven P, Reason C (2016) Annual cycle of the upper-ocean dynamics in the tropical western Indian Ocean and influences on regional ocean properties. African Journal of Marine Science 38 (1): 81-99 [doi:10.2989/1814232X.2016.1158123]

Marchesiello P, McWilliams JC, Shchepetkin A (2001) Open boundary condition for long-term integration of regional oceanic models. Ocean Model 3: 1-21 [https://doi.org/10.1016/S1463-5003(00)00013-5]

Meehl GA, Arblaster JM, Fasullo JT, Hu A, Trenberth KE (2011) Model-based evidence of deep-ocean heat uptake during surface-temperature hiatus periods. Nature Climate Change 1: 360-364 [doi.org/10.1038/nclimate1229]

Nieves V, Willis JK, Patzert WC (2015) Recent hiatus caused by decadal shift in Indo-Pacific heating. Science 349: 532-535 [doi.org/10.1126/science. aaa4521]

Obura D, Celliers L, Machano H, Mangubhai S, Mohammed M, Motta H, Muhando C, Muthiga N, Pereira M, Schleyer M (2002) Status of coral reefs in Eastern Africa: Kenya, Tanzania, Mozambique and South Africa. In: Wilkinson C (ed) Status of coral reefs of the world, 2002. Global Coral Reef Monitoring Network (GCRMN). Australian Institute of Marine Science, Townsville, Australia. pp 63-78

Penven P, Lutjeharms JRE, Florenchie P (2006) Madagascar: A pacemaker for the Agulhas Current system? Geophysical Research Letters 33: L17609 [doi:10.1029/2006GL026854]

Pierce DW, Barnett TP, AchutaRao KM, Gleckler PJ, Gregory JM, Washington WM (2006) Anthropogenic warming of the oceans: observations and model results. Journal of Climate 19: 1873-1900 [doi.org/10.1175/JCLI3723.1]

Rao SA, Behera SK, Masumoto Y, Yamagata T (2002) Interannual variability in the subsurface tropical Indian Ocean. Deep-Sea Research II 49: 1549-1572 [https://doi.org/10.1016/S0967-0645(01)00158-8]

Rao SA, Behera SK (2005) Subsurface influence on SST in the tropical Indian Ocean: Structure and inter-annual variability. Dynamics of Atmospheres and Oceans 39: 103-135 [https://doi.org/10.1016/j.dynatmoce.2004.10.014]

Reason CJC, Allan RJ, Lindesay JA, Ansell T (2000) ENSO and climatic signals across the Indian Ocean basin in the global context: Part 1, Inter-annual composite patterns. International Journal of Climatology 20: 1285-1327 [https://doi.org/10.1002/1097-0088(200009)20:11<1285::AID-JOC536>3.0.CO;2-R]

Saji N, Goswami B, Vinayachandran P, Yamagata T (1999) A dipole mode in the Tropical Ocean. Nature 401: 360–363 [doi.org/10.1038/43854]

Sayantani O, Gnanaseelan C (2015) Tropical Indian Ocean subsurface temperature variability and the forcing mechanisms. Climate Dynamics 44: 2447-2462 [doi.org/10.1007/s00382-014-2379-y]

Schott FA, Xie SP, McCreary Jr JP (2009) Indian Ocean circulation and climate variability. Reviews of Geophysics 47: RG1002 [doi:10.1029/2007RG000245]

Shchepetkin A, McWilliams J (2003) A method for computing horizontal pressure-gradient force in an ocean model with a non-aligned vertical coordinate. Journal of Geophysical Research 108: 35.1-35.34 [https://doi.org/10.1029/2001JC001047]

Shchepetkin A, McWilliams J (2005) The Regional Oceanic Modelling System (ROMS): A split-explicit, free-surface, topography following coordinate oceanic model. Ocean Modelling 9: 347-404 [https://doi.org/10.1016/j.ocemod.2004.08.002]

Shinoda T, Hendon HH, Alexander MA (2004) Surface and subsurface dipole variability in the Indian Ocean and its relation with ENSO. Deep Sea Research Part I: Oceanography Research Papers 51: 619-635 [doi.org/10.1016/j.dsr.2004.01.005]

Smith WHF, Sandwell DT (1997) Global seafloor topography from satellite altimetry and ship depth soundings. Science 277: 1957-1962 [doi: 10.1126/science.277.5334.1956]

Sun S, Fang Y, Liu L, Wang H, Liu Y, Zhang M (2021) Regime shift in the decadal variability of the Indian Ocean subsurface temperature. Journal of Marine Systems 216: 103511 [ISSN 0924-7963] [doi.org/10.1016/j.jmarsys.2021.103511]

Tozuka T, Yokoi T, Yamagata T (2010) A modeling study of interannual variations of the Seychelles Dome. Journal of Geophysical Research 115: C04005 [doi:10.1029/2009JC005547]

Trenary LL, Han W (2008) Causes of decadal subsurface cooling in the tropical Indian Ocean during 1961-2000. Geophysical Research Letters 35: L17602 [doi.org/10.1029/ 2008GL034687]

Vecchi GA, Harrison DE (2013) Interannual Indian rainfall variability and Indian Ocean sea surface temperature anomalies. Geophysical Monograph Series: 247-259 [doi.org/10.1029/147GM14]

Xie SP, Annamalai H, Schott FA, McCreary J P (2002) Structure and mechanism of South Indian Ocean climate variability. Journal of Climate 15: 864-878 [doi: https://doi.org/10.1175/1520-0442(2002)015<0864:SAMOSI>2.0.CO;2]

Yamagata T, Behera SK, Luo JJ, Masson S, Jury MR, Rao SA (2004) Coupled ocean–atmosphere variability in the tropical Indian Ocean. In: Wang C (ed) Earth's climate: The ocean-atmosphere interaction. Geophysical Monograph Series 147: 189-212 [doi: 10.1029/147GM12]

Yokoi T, Tozuka T, Yamagata T (2008) Seasonal variation of the Seychelles Dome. Journal of Climate 21: 3740-3754 [https://doi.org/10.1175/2008JCLI1957.1]

Yokoi T, Tozuka T, Yamagata T (2012) Seasonal and interannual variations of the SST above the Seychelles Dome. Journal of Climate 25: 800-814 [doi.org/10.1175/JCLI-D-10- 05001.1]

Yu W, Xiang B, Liu L, Liu N (2005) Understanding the origins of inter-annual thermocline variations in the tropical Indian Ocean. Geophysical Research Letters 32: L24706 [doi: 10.1029/2005GL024327]